

Effects of weak point disorder on the vortex matter phase diagram in untwinned $\text{YBa}_2\text{Cu}_3\text{O}_y$ single crystals

Terukazu Nishizaki*

*Institute for Materials Research, Tohoku University, Sendai 980-8577, Japan
and CREST, Japan Science and Technology Corporation, Kawaguchi 332-0012, Japan*

Tomoyuki Naito[†]

Institute for Materials Research, Tohoku University, Sendai 980-8577, Japan

Satoru Okayasu and Akihiro Iwase

Japan Atomic Energy Research Institute, Ibaraki 319-1195, Japan

Norio Kobayashi

*Institute for Materials Research, Tohoku University, Sendai 980-8577, Japan;
CREST, Japan Science and Technology Corporation, Kawaguchi 332-0012, Japan;
and Center for Low Temperature Science, Tohoku University, Sendai 980-8577, Japan*

(Received 25 May 1999; revised manuscript received 13 September 1999)

Effects of the weak point disorder on the vortex matter phase diagram are studied by an irradiation of 2.5 MeV electrons in untwinned $\text{YBa}_2\text{Cu}_3\text{O}_y$ single crystals. We find that the point disorder lowers the critical point H_{cp} of the first-order vortex lattice melting line $H_{\text{m}}(T)$ and has an opposite effect on the vortex glass phase boundary above and below H_{cp} . Below H_{cp} , the field-driven disordering transition line $H^*(T)$ between the Bragg glass and the vortex glass phases shifts to lower fields and the vortex glass phase is expanded after irradiation. Near the vortex liquid-to-glass transition line $H_{\text{g}}(T)$ above H_{cp} , on the other hand, the vortex glass phase is reduced after irradiation, indicating the enhanced vortex wandering by the point disorder in the critical region.

In the mixed state of high-temperature superconductors, it has been demonstrated that the vortex solid in clean systems undergoes a first-order melting transition into the vortex liquid due to strong thermal fluctuations.¹⁻⁸ The vortex lattice melting line $H_{\text{m}}(T)$ terminates^{7,9} at a critical point H_{cp} and changes to a continuous second-order vortex glass^{9,10} transition line $H_{\text{g}}(T)$ above H_{cp} . Recent experiments¹¹⁻²⁰ have shown that the vortex matter phase diagram is more complicated and the vortex solid is divided into at least two distinct phases by a characteristic field $H^*(T)$ at which the positional correlations of the vortex lattice are significantly reduced^{11,12} and the magnetization shows steep increase toward the second peak in $\text{Bi}_2\text{Sr}_2\text{CaCu}_2\text{O}_8$,^{13,14} $\text{YBa}_2\text{Cu}_3\text{O}_y$,¹⁶⁻¹⁹ and $\text{Nd}_{1.85}\text{Ce}_{0.15}\text{CuO}_4$.²⁰ These results are supported by both several theoretical studies²¹⁻²⁵ and numerical simulations,²⁶ and $H^*(T)$ is interpreted as the field-driven disordering transition line between a relatively ordered vortex lattice (or the Bragg glass) phase at low fields and a highly disordered vortex glass phase at high fields. The stability of the Bragg glass phase with quasi-long-range translational order and the nature of the vortex system are determined by the delicate balance between three energies,²¹⁻²⁶ namely, the vortex elastic energy E_{el} , the vortex pinning energy E_{pin} , and the thermal energy E_{th} . Therefore, the degree of the disorder in the system related to the value of E_{pin} is an important parameter to understand details of the vortex matter phase diagram.

Fendrich *et al.*²⁷ have reported that the first-order vortex lattice melting transition in untwinned $\text{YBa}_2\text{Cu}_3\text{O}_y$ was de-

stroyed by the introduction of the point disorder by the electron irradiation. Although the increase of viscosity of the vortex liquid has been discussed in terms of the vortex entanglement,²⁷ the effect of the point disorder on both the field-driven disordering transition line $H^*(T)$ in the vortex solid phase and the vortex glass transition line $H_{\text{g}}(T)$ above H_{cp} remains unanswered.

In this paper, we investigate effects of the electron irradiation on the vortex matter phase diagram and on three transition lines of $H_{\text{m}}(T)$, $H_{\text{g}}(T)$, and $H^*(T)$ in untwinned $\text{YBa}_2\text{Cu}_3\text{O}_y$. We find an opposite effect on the vortex glass phase boundary above and below H_{cp} . We show that H_{cp} and $H^*(T)$ shift to lower fields and the vortex glass phase is stabilized by the introduced point disorder below H_{cp} . These results give a strong support for the field-driven disordering transition scenario.²¹⁻²⁶ We also present that $H_{\text{g}}(T)$ above H_{cp} shifts to lower temperatures and the vortex glass phase is reduced after irradiation, indicating the enhanced vortex fluctuations in the critical region.

$\text{YBa}_2\text{Cu}_3\text{O}_y$ single crystals were grown by a self-flux method using yttria crucibles and were detwinned by annealing at 450 °C under a uniaxial pressure.²⁸ According to the relation between a doping level and an annealing temperature,²⁹ a sample in this study was a slightly overdoped single crystal of untwinned $\text{YBa}_2\text{Cu}_3\text{O}_y$. The untwinned single crystal with dimensions of $0.66 \times 0.55 \times 0.07$ mm³ showed a superconducting transition at $T_{\text{c}} \approx 92$ K. A Hall probe magnetometry was performed by measuring the

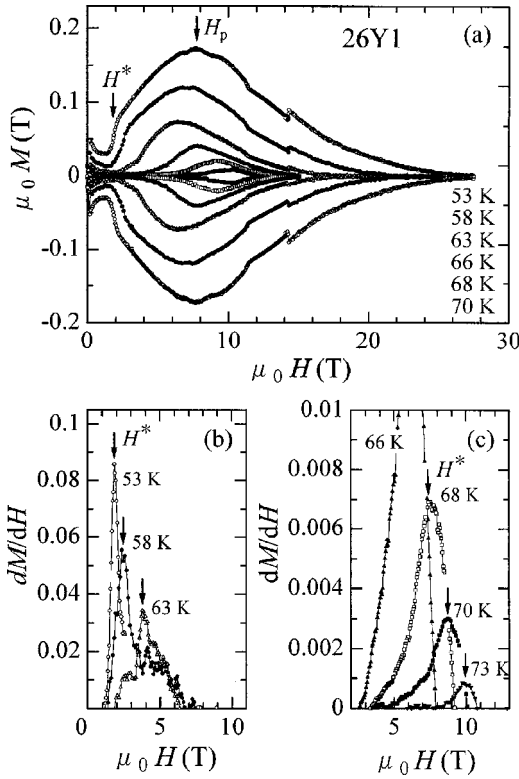


FIG. 1. (a) Magnetization curves of untwinned $\text{YBa}_2\text{Cu}_3\text{O}_y$ before electron irradiation. A characteristic field H^* is defined by a sharp peak in the magnetic-field derivative dM/dH at (b) low temperatures and (c) high temperatures.

magnetic flux density at the center and the outside of the sample using two Hall probes.¹⁶ The resistivity ρ was measured by dc four-probe method using a Keithley 2001 multimeter and a Keithley 1801 preamplifier with a noise level of ~ 0.1 nV under a current density $J \approx 1$ A/cm². The magnetic field ($H \parallel$ the c axis) up to 27 T was generated by a hybrid magnet system at High Field Laboratory for Superconducting Materials, IMR, Tohoku University. An irradiation of 2.5 MeV electrons was performed with the Dynamitron electron accelerator in JAERI at Takasaki. A very low dose (1×10^{18} e/cm²) of electron irradiation was chosen to study the effect of weak point disorder on the vortex matter phase diagram; the value is an order of magnitude smaller than the one of the previous study.²⁷ Since the irradiation and the measurement were repeated twice using the same crystal, the total irradiation dose was 2×10^{18} e/cm². The T_c change after the second irradiation was $\Delta T_c \sim 0.4$ K.

Figure 1(a) shows the magnetization (M - H) curves of untwinned $\text{YBa}_2\text{Cu}_3\text{O}_y$ before electron irradiation. The magnetization shows a step increase at a characteristic field H^* and a remarkable second peak at H_p . As shown in Figs. 1(b) and 1(c), H^* is defined by a sharp peak in the magnetic-field derivative dM/dH , indicating the drastic change of the vortex state. The steep increase of the magnetization at H^* is remarkable in the local magnetization measurements,^{13,16,19,20} as compared with the bulk magnetization measurements.^{17,18} Although the peak in dM/dH becomes broader in the high-temperature region near the critical point due to the thermal smearing effect, H^* still behaves as a characteristic field such as the onset of the broad second

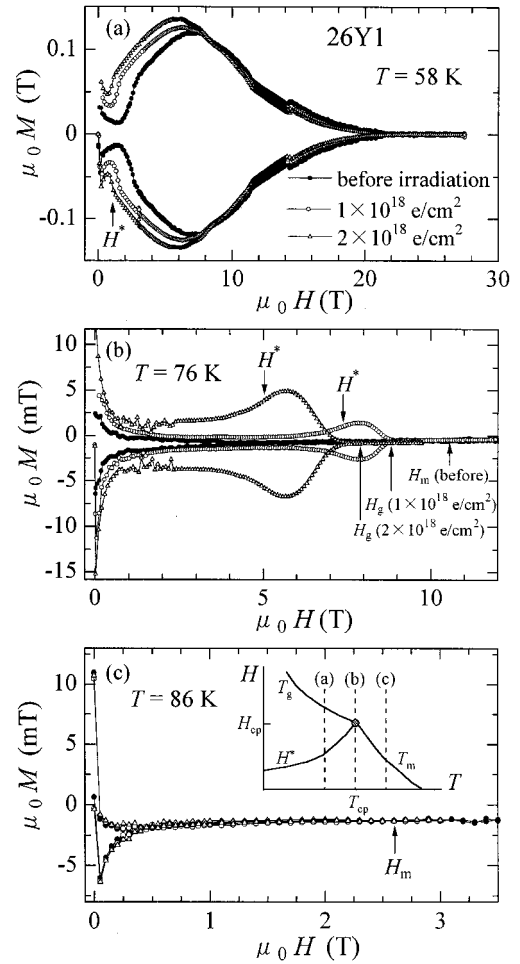


FIG. 2. Magnetization curves of untwinned $\text{YBa}_2\text{Cu}_3\text{O}_y$ before and after electron irradiation with different irradiation doses for three different temperatures: (a) $T < T_{cp}$, (b) $T \approx T_{cp}$, and (c) $T > T_{cp}$. Inset: Schematic drawing of the measured temperature region in the H - T phase diagram.

peak. In addition, a partial magnetization loop technique has been applied to the broad second peak recently and it is concluded that the onset of the second peak corresponds to the field-driven disordering transition line.¹⁸ With increasing temperature, $H_p(T)$ and $H^*(T)$ increase and terminate at the critical point ($\mu_0 H_{cp} \approx 11$ T) of the first-order vortex lattice melting line as mentioned below.

The magnetization curves in Fig. 1(a) show an additional structure around 14.5 T. In our hybrid magnet system, the magnetic field is applied by using the superconducting magnet below 14.5 T and the field by the water-cooled magnet is superposed above 14.5 T. The sweep rate of the superconducting magnet is reduced in the field range 11.5–14.5 T and a sweep rate (≈ 10 mT/s) of the water-cooled magnet is about two times larger than that of the superconducting magnet. Therefore, the additional structure around 14.5 T results from the relaxation effect due to the different sweep rate.

Figure 2 shows M - H curves of untwinned $\text{YBa}_2\text{Cu}_3\text{O}_y$ before and after electron irradiation with different irradiation dose. The electron irradiation effect on the magnetization strongly depends on the temperature region which is characterized by a temperature T_{cr} of the critical point on the first-order vortex lattice melting line. The inset of Fig. 2(c) shows

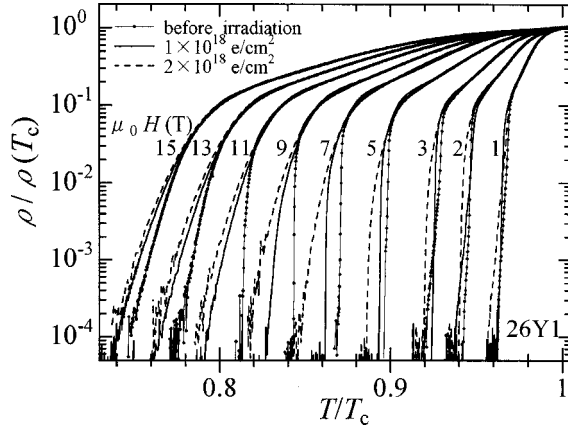


FIG. 3. Normalized resistivity versus temperature in untwinned $\text{YBa}_2\text{Cu}_3\text{O}_y$ before and after electron irradiation.

a schematic drawing of measured temperatures in the H - T phase diagram. Figure 2(a) shows magnetization curves in the low-temperature region below $T_{\text{cp}} \approx 75.5$ K. With increasing irradiation dose, H^* and H_p shift to lower-field region and the jump height of the magnetization at H^* becomes smaller. The hysteresis width in the magnetization curve, which is proportional to the critical current density, increases after irradiation in the low-field region below H_p , however it slightly decreases above H_p .

In the intermediate-temperature region near T_{cp} , the characteristic feature in the magnetization changes drastically before and after irradiation as shown in Fig. 2(b). Before irradiation, the magnetization decreases monotonically with increasing field and the irreversibility field H_{irr} is much smaller than the vortex lattice melting field H_m , similarly to previous results.^{3,5,16} Melting fields H_m and H_g expressed by arrows in Fig. 2 were derived from the resistivity measurement as mentioned below. After irradiation, however, the second peak appears just below H_g and the magnetization shows the irreversible property up to H_g . Although H_{irr} and H_g decrease with increasing point disorder, the hysteresis width increases, indicating the enhanced pinning force after irradiation in the vortex solid phase.

In the high-temperature region above T_{cp} [see Fig. 2(c)], the magnetization shows reversible property in the wide field region below H_m . Since the magnetization hysteresis is independent of the irradiation dose, the introduced point disorder is not effective as the pinning center. The extremely weak vortex pinning above T_{cp} is related to the anomalous irreversibility line¹⁶ due to the thermal smearing effect on the disordered potential¹ or the depinning transition.^{15,30}

Figure 3 shows the normalized resistivity $\rho/\rho(T_c)$ versus temperature T/T_c before and after electron irradiation. The unirradiated sample shows the sharp resistive drop due to the first-order vortex lattice melting transition below $\mu_0 H_{\text{cp}} \approx 11$ T. Although the vortex lattice melting transition remains after irradiation in the low-field region, the transition temperature $T_m(H)$ slightly shifts to lower temperatures. The behavior is contrary to the results by Fendrich *et al.*²⁷ who have reported that the vortex lattice melting transition was completely destroyed by the electron irradiation with a dose of $1 \times 10^{19} \text{ e/cm}^2$; the value is an order of magnitude larger than one in this study. In the vortex liquid phase just above

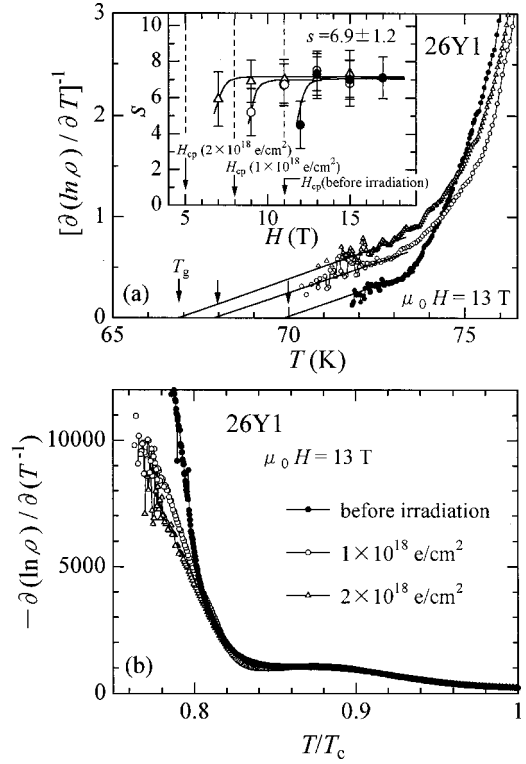


FIG. 4. (a) The inverse logarithmic derivative of the resistivity at 13 T in the vicinity of the vortex glass transition temperature T_g before and after electron irradiation. Inset: Magnetic-field dependence of the critical exponent s above H_{cp} . The solid curves are guides to the eye. (b) Reduced temperature dependence of the activation energy at 13 T before and after electron irradiation.

T_m , the resistivity decreases after irradiation^{27,31} because the viscosity in the vortex liquid increases by the introduced point disorder.

Above the critical point H_{cp} , the signature of the first-order melting transition disappears and the transition becomes the second-order glassy transition. The vortex glass theory¹⁰ predicts the temperature dependence of the linear resistivity $\rho(T) \propto (T - T_g)^s$ near the glass transition temperature T_g , where s is the critical exponent. As shown in Fig. 4(a), the linear resistivity above H_{cp} is well described by this equation and a plot of $[\partial(\ln \rho)/\partial T]^{-1}$ versus T shows a straight line in the critical region of the glass transition.¹⁰ The inset of Fig. 4(a) shows the critical exponent s as a function of the magnetic field above H_{cp} before and after electron irradiation. The critical exponent obtained from the slope $1/s$ in Fig. 4(a) is independent of both magnetic field and irradiation dose in the high-field region well above H_{cp} , except for the slightly smaller value of s in the vicinity of H_{cp} . The averaged value of the critical exponent $s = 6.9 \pm 1.2$ in high fields is consistent with the previously reported value for single crystals of untwinned $\text{YBa}_2\text{Cu}_3\text{O}_y$ ($s = 6 - 7 \pm 1$),^{9,32} twinned $\text{YBa}_2\text{Cu}_3\text{O}_y$ ($s = 6.5 \pm 1.5$),³³ and $\text{Bi}_2\text{Sr}_2\text{CaCu}_2\text{O}_y$ ($s = 7 \pm 1$).³⁴ The result agrees well with the vortex glass theory,¹⁰ so vortices in the liquid phase are frozen into the vortex glass phase with decreasing temperature. Contrary to the above result, earlier experiments on untwinned $\text{YBa}_2\text{Cu}_3\text{O}_y$ irradiated by electron²⁷ and proton^{35,36} did not show evidence of the vortex glass transition and the field-dependent critical exponent ($1.2 < s < 4.5$) was

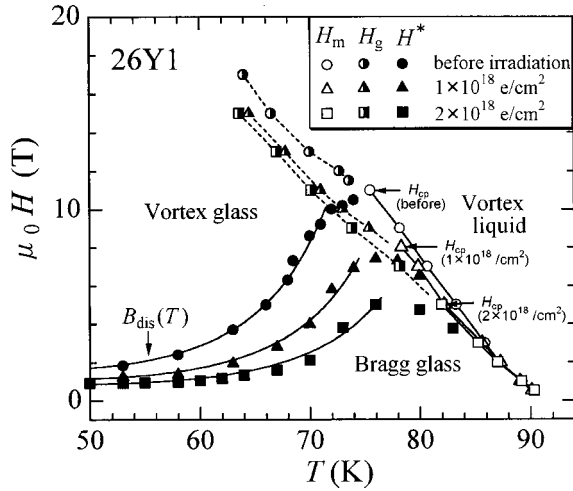


FIG. 5. Vortex matter phase diagram in untwinned $\text{YBa}_2\text{Cu}_3\text{O}_y$ before and after electron irradiation. Three different phases, i.e., the vortex liquid, the vortex glass, and the Bragg glass, are divided by transition lines $H_m(T)$, $H_g(T)$, and $H^*(T)$. The solid curves are fit to the field-driven transition line $B_{\text{dis}}(T)$.

observed.^{27,35} However, Petrean *et al.*³⁷ have recently suggested that there is a threshold of the pinning disorder and the sufficiently large pinning is required in order to observe the vortex glass transition with the universal critical exponent; the result by proton irradiation³⁷ is consistent with the present study [see inset of Fig. 4(a)] because the obtained critical exponent increases only in low fields near H_{cp} and becomes constant with increasing effective disorder in high fields. In addition, the activation energy U_0 (≈ 1000 K at 13 T) for untwinned $\text{YBa}_2\text{Cu}_3\text{O}_y$ in this study, which is shown below [see Fig. 4(b)], is larger than that in previous reports.^{27,35} These results indicate that the vortex glass transition with the field-independent critical exponent is observable when the disorder density and the applied magnetic field are higher; this situation has been predicted by the recent theory.³⁸

The vortex glass transition temperature T_g determined by the extrapolation [see Fig. 4(a)] decreases after irradiation. At $\mu_0 H = 13$ T, for example, T_g decreases, $\Delta T_g \sim 3$ K, after the second electron irradiation; the value is considerably larger than $\Delta T_g \sim 0.4$ K. Figure 4(b) shows the local slope in the Arrhenius plots $-\partial(\ln \rho)/\partial(T^{-1})$, namely the activation energy U , as a function of the reduced temperature before and after electron irradiation. With decreasing temperature, the activation energy shows a plateau^{34,35} with a value of $U_0 \approx 1000$ K and changes to a divergent behavior below $T/T_c \sim 0.82$, indicating the crossover from the Arrhenius to the vortex glass regime. Although the crossover temperature is almost disorder independent, the divergence of the activation energy is suppressed by the irradiation. Therefore the critical region of the vortex glass transition is enhanced by the point disorder introduced by electron irradiation. In the low-field region near H_{cp} , however, the critical region of the vortex glass transition becomes narrower, so the measured resistivity cannot reach the critical region because of the limited accuracy; in this case, the estimated value of s would be unreliable.

Figure 5 shows the magnetic field versus temperature phase diagram in untwinned $\text{YBa}_2\text{Cu}_3\text{O}_y$ before and after

electron irradiation. The vortex matter phase diagram remarkably depends on the irradiation dose near the critical point. The characteristic fields $H^*(T)$, $H_g(T)$, and H_{cp} shift to lower-field region with increasing point disorder, however, three transition lines of $H^*(T)$, $H_g(T)$, and $H_m(T)$ always terminate at the critical point independently of the irradiation dose. The vortex matter phase diagram before irradiation is discussed in a previous paper¹⁶ and $H^*(T)$ connected with H_{cp} is interpreted as a field-driven disordering transition line^{21–26} between the vortex glass phase and the topologically ordered Bragg glass phase with quasi-long-range translational order. Beyond the disordering transition line, dislocations are induced by the randomly distributed disorder and the Bragg glass phase undergoes a transition into the disordered vortex glass phase. In the Bragg glass phase, elasticity of vortices is strong, so the volume pinning force is reduced. In the vortex glass phase, on the other hand, vortices have an additional effective degree of freedom due to free dislocations and can adapt more easily to the pinning potential, indicating the strong volume pinning force. Therefore, the magnetization and the critical current density show steep increase at the field-driven disordering transition line. Since the Bragg glass is the almost perfect vortex lattice as far as translational order is concerned in spite of a finite pinning force, it is reasonable that the Bragg glass phase is suppressed and the vortex glass phase is enhanced by the introduced point disorder as predicted in recent theories.^{21–26}

As mentioned above, the field-driven disordering transition line $H^*(T)$ is connected with the critical point T_{cp} and divides the vortex solid into two regions. However, in the high-temperature region above T_{cp} , $H^*(T)$ turns down and meets the vortex lattice melting line $H_m(T)$ below H_{cp} for irradiated $\text{YBa}_2\text{Cu}_3\text{O}_y$. This feature is observed only in the crystal with relatively strong pinning force, because $H^*(T)$ disappears at T_{cp} for unirradiated $\text{YBa}_2\text{Cu}_3\text{O}_y$. Since $H^*(T)$ above T_{cp} decreases along $H_m(T)$ and disappears, the second peak effect just below $H_m(T)$ is closely related to the enhanced vortex pinning due to the vortex lattice softening prior to the vortex lattice melting as reported previously.^{39–41} These results indicate that $H^*(H)$ merges with both $H_m(T)$ and the premelting peak effect at the critical point for irradiated $\text{YBa}_2\text{Cu}_3\text{O}_y$. The region between $H^*(T)$ and $H_m(T)$ above T_{cp} is very narrow in the present study, so the result above mentioned is completely different from the recently reported second peak^{29,42} which intersects $H_m(T)$ well below H_{cp} for optimally doped and slightly underdoped $\text{YBa}_2\text{Cu}_3\text{O}_y$.

Applying the Lindemann-type criterion,^{22,23} temperature dependence of the disordering transition line is given by $B_{\text{dis}}(T) \approx B_{\text{dis}}(0)(T_{\text{dp}}^{\text{s}}/T)^{10/3} \exp[(2c/3)(T/T_{\text{dp}}^{\text{s}})^3]$ for $T > T_{\text{dp}}^{\text{s}}$. Here, T_{dp}^{s} is the single vortex depinning temperature,¹ c a constant of order unity,¹ and $B_{\text{dis}}(0)$ the transition field for $T \ll T_{\text{dp}}^{\text{s}}$. The disordering transition line increases exponentially in the high- T region, because the smoothing of the quenched disorder potential by thermal fluctuations becomes greater above the depinning line.¹ As shown by the solid curves in Fig. 5, the experimentally determined $H^*(T)$ agrees well with this model using the reasonable parameters, $B_{\text{dis}}(0) \approx 0.93, 0.65,$ and 0.5 T and $T_{\text{dp}}^{\text{s}} \approx 37.8, 39.2,$ and 40.5 K for unirradiated, first-irradiated, and second-irradiated

samples, respectively. In a previous paper¹⁶ the value of $B_{\text{dis}}(0)$ is estimated to be 1–6 T using the parameters for $\text{YBa}_2\text{Cu}_3\text{O}_y$ and the reduction of $B_{\text{dis}}(0)$ is expected with increasing disorder.^{21–26} Both decrease in $B_{\text{dis}}(0)$ and increase in T_{dp}^{s} are consistent with the enhanced vortex pinning after electron irradiation. Therefore, the vortex glass phase is stabilized by the introduction of the point disorder and the strong pinning region is expanded to the lower fields. These results of electron irradiation effect provide further evidence of the field-driven disordering transition scenario^{21–26} as a possible origin of $H^*(T)$, which have been discussed in previous papers.^{14–20}

The reduction of the vortex glass transition line $H_{\text{g}}(T)$ and the increase of the critical region after irradiation result from the enhanced vortex fluctuations by the introduced point disorder. Since the randomly distributed point disorder induces vortex wandering, the vortex liquid phase and the vortex entangled state³⁵ are stabilized by the combination effect of the thermal and disorder fluctuations in the critical region of the vortex glass. The vortex glass transition as a function of the pinning strength is discussed theoretically²⁵ and the decrease of T_{g} with increasing point disorder is expected for the system with weak pinning. Thus, the electron irradiation effect on the vortex glass transition temperature is consistent with the recent theory.²⁵ In addition, the behavior of $H_{\text{g}}(T)$ after electron irradiation is different from the heavy-ion irradiation effect, because the correlated disorder

suppresses the vortex fluctuations and $H_{\text{g}}(T)$ increases with increasing columnar defect. These results indicate that effects of the introduced point disorder depend on the region of the vortex matter phase diagram; the vortex pinning force increases and the Bragg glass phase is suppressed near the field-driven disordering transition line $H^*(T)$ below H_{cp} , and the vortex liquid is enhanced near the vortex glass transition line $H_{\text{g}}(T)$ above H_{cp} .

In conclusion, we have investigated the electron irradiation effect on the vortex matter phase diagram in untwinned $\text{YBa}_2\text{Cu}_3\text{O}_y$. We have found that the vortex matter phase diagram is drastically changed near H_{cp} and $H^*(T)$ connected with H_{cp} shifts to lower fields by the point disorder, indicating the reduction of the Bragg glass phase, i.e., the enhancement of the vortex glass phase. These results provide further evidence of the field-driven disordering transition scenario. We have shown the opposite effect on the vortex glass phase boundary that $H_{\text{g}}(T)$ above H_{cp} shifts to lower temperatures and the vortex glass phase is reduced by the point disorder due to enhanced vortex wandering in the critical region.

The authors would like to thank T. Nojima, R. Ikeda, X. Hu, K. Shibata, T. Sasaki, K. Watanabe, and S. Awaji for valuable discussions, and A. M. Petrean for sending a copy of her unpublished work. Part of this work was carried out at the HFLSM, IMR, Tohoku University. We thank K. Sai, Y. Ishikawa, and Y. Sasaki of HFLSM.

*Electronic address: terukazu@imr.tohoku.ac.jp

[†]Present address: School of Materials Science, Japan Advanced Institute of Science and Technology, Tatsunokuchi 923-1292, Japan.

¹G. Blatter, M. V. Feigel'man, V. B. Geshkenbein, A. I. Larkin, and V. M. Vinokur, *Rev. Mod. Phys.* **66**, 1125 (1994).

²H. Safar, P. L. Gammel, D. A. Huse, D. J. Bishop, J. P. Rice, and D. M. Ginsberg, *Phys. Rev. Lett.* **69**, 824 (1992); W. K. Kwok, S. Fleshler, U. Welp, V. M. Vinokur, J. Downey, G. W. Crabtree, and M. M. Miller, *ibid.* **69**, 3370 (1992).

³R. Liang, D. A. Bonn, and W. N. Hardy, *Phys. Rev. Lett.* **76**, 835 (1996).

⁴T. Nishizaki, Y. Onodera, T. Naito, and N. Kobayashi, *J. Low Temp. Phys.* **105**, 1183 (1996).

⁵U. Welp, J. A. Fendrich, W. K. Kwok, G. W. Crabtree, and B. W. Veal, *Phys. Rev. Lett.* **76**, 4809 (1996).

⁶A. Schilling, R. A. Fisher, N. E. Phillips, U. Welp, D. Dasgupta, W. K. Kwok, and G. W. Crabtree, *Nature (London)* **382**, 791 (1996); A. Junod, M. Roulin, J. Y. Genoud, B. Revaz, A. Erb, and E. Walker, *Physica C* **275**, 245 (1997); M. Roulin, A. Junod, A. Erb, and E. Walker, *Phys. Rev. Lett.* **80**, 1722 (1998).

⁷H. Pastoriza, M. F. Goffman, A. Arribère, and F. de la Cruz, *Phys. Rev. Lett.* **72**, 2951 (1994); E. Zeldov, D. Majer, M. Konczykowski, V. B. Geshkenbein, V. M. Vinokur, and H. Shtrikman, *Nature (London)* **375**, 373 (1995).

⁸X. Hu, S. Miyashita, and M. Tachiki, *Phys. Rev. Lett.* **79**, 3498 (1997).

⁹H. Safar, P. L. Gammel, D. A. Huse, D. J. Bishop, W. C. Lee, J. Giapintzakis, and D. M. Ginsberg, *Phys. Rev. Lett.* **70**, 3800 (1993); H. Safar, P. L. Gammel, D. A. Huse, G. B. Alers, D. J. Bishop, W. C. Lee, J. Giapintzakis, and D. M. Ginsberg, *Phys. Rev. B* **52**, 6211 (1995).

¹⁰M. P. A. Fisher, *Phys. Rev. Lett.* **62**, 1415 (1989); D. S. Fisher,

M. P. A. Fisher, and D. A. Huse, *Phys. Rev. B* **43**, 130 (1991).

¹¹R. Cubitt, E. M. Forgan, G. Yang, S. L. Lee, D. Mck. Paul, H. A. Mook, M. Yethiraj, P. H. Kes, T. W. Li, A. A. Menovsky, Z. Tarnawski, and K. Mortensen, *Nature (London)* **365**, 407 (1993).

¹²S. L. Lee, P. Zimmermann, H. Keller, M. Warden, I. M. Savić, R. Schauwecker, D. Zech, R. Cubitt, E. M. Forgan, P. H. Kes, T. W. Li, A. A. Menovsky, and Z. Tarnawski, *Phys. Rev. Lett.* **71**, 3862 (1993).

¹³B. Khaykovich, E. Zeldov, D. Majer, T. W. Li, P. H. Kes, and M. Konczykowski, *Phys. Rev. Lett.* **76**, 2555 (1996).

¹⁴B. Khaykovich, M. Konczykowski, E. Zeldov, R. A. Doyle, D. Majer, P. H. Kes, and T. W. Li, *Phys. Rev. B* **56**, R517 (1997).

¹⁵D. T. Fuchs, E. Zeldov, T. Tamegai, S. Ooi, M. Rappaport, and H. Shtrikman, *Phys. Rev. Lett.* **80**, 4971 (1998).

¹⁶T. Nishizaki, T. Naito, and N. Kobayashi, *Phys. Rev. B* **58**, 11 169 (1998); *Physica C* **282-287**, 2117 (1997); **317-318**, 645 (1999).

¹⁷K. Deligiannis, P. A. J. de Groot, M. Oussena, S. Pinfold, R. Langan, R. Gangon, and L. Taillefer, *Phys. Rev. Lett.* **79**, 2121 (1997); H. Küpfer, Th. Wolf, C. Lessing, A. A. Zhukov, X. Lancon, R. Meier-Hirmer, W. Schauer, and H. Wühl, *Phys. Rev. B* **58**, 2886 (1998); S. Okayasu and H. Asaoka, *Physica C* **317-318**, 633 (1999).

¹⁸S. Kokkaliaris, P. A. J. de Groot, S. N. Gordeev, A. A. Zhukov, R. Gagnon, and L. Taillefer, *Phys. Rev. Lett.* **82**, 5116 (1999).

¹⁹D. Giller, A. Shaulov, Y. Yeshurun, and J. Giapintzakis, *Phys. Rev. B* **60**, 106 (1999).

²⁰D. Giller, A. Shaulov, R. Prozorov, Y. Abulafia, Y. Wolfus, L. Burlachkov, Y. Yeshurun, E. Zeldov, V. M. Vinokur, J. L. Peng, and R. L. Greene, *Phys. Rev. Lett.* **79**, 2542 (1997).

²¹T. Giamarchi and P. Le. Doussal, *Phys. Rev. Lett.* **72**, 1530

- (1994); Phys. Rev. B **52**, 1242 (1995); **55**, 6577 (1997).
- ²²D. Ertas and D. R. Nelson, Physica C **272**, 79 (1996).
- ²³J. Kierfeld, Physica C **300**, 171 (1998).
- ²⁴D. Carpentier, P. Le. Doussal, and T. Giamarchi, Europhys. Lett. **35**, 379 (1996); J. Kierfeld, T. Nattermann, and T. Hwa, Phys. Rev. B **55**, 626 (1997); D. S. Fisher, Phys. Rev. Lett. **78**, 1964 (1997); Y. Y. Goldschmidt, Phys. Rev. B **56**, 2800 (1997); V. Vinokur, B. Khaykovich, E. Zeldov, M. Konczykowski, R. A. Doyle, and P. H. Kes, Physica C **295**, 209 (1998).
- ²⁵R. Ikeda, J. Phys. Soc. Jpn. **65**, 3998 (1996).
- ²⁶M. J. P. Gingras and D. A. Huse, Phys. Rev. B **53**, 15 193 (1996); S. Ryu, A. Kapitulnik, and S. Doniach, Phys. Rev. Lett. **77**, 2300 (1996); A. Otterlo, R. T. Scalettar, and G. T. Zimányi, *ibid.* **81**, 1497 (1998).
- ²⁷J. A. Fendrich, W. K. Kwok, J. Giapintzakis, C. J. van der Beek, V. M. Vinokur, S. Fleshler, U. Welp, H. K. Viswanathan, and G. W. Crabtree, Phys. Rev. Lett. **74**, 1210 (1995).
- ²⁸T. Naito, T. Nishizaki, Y. Watanabe, and N. Kobayashi, in *Advances in Superconductivity IX*, edited by S. Nakajima and M. Murakami (Springer-Verlag, Tokyo, 1997), p. 601.
- ²⁹T. Nishizaki, K. Shibata, T. Naito, M. Maki, and N. Kobayashi, J. Low Temp. Phys. (to be published).
- ³⁰B. Horovitz and T. R. Goldin, Phys. Rev. Lett. **80**, 1734 (1998).
- ³¹T. Nishizaki, T. Naito, S. Okayasu, A. Iwase, and N. Kobayashi, in *Advances in Superconductivity XI*, edited by N. Koshizuka and S. Tajima (Springer-Verlag, Tokyo, 1999), p. 585.
- ³²T. Naito, T. Nishizaki, and N. Kobayashi, Physica C **293**, 186 (1997).
- ³³P. L. Gammel, L. F. Schneemeyer, and D. J. Bishop, Phys. Rev. Lett. **66**, 953 (1991).
- ³⁴H. Safar, P. L. Gammel, D. J. Bishop, D. B. Mitzi, and A. Kapitulnik, Phys. Rev. Lett. **68**, 2672 (1992).
- ³⁵D. López, L. Krusin-Elbaum, H. Safar, E. Righi, F. de la Cruz, S. Grigera, C. Feild, W. K. Kwok, L. Paulis, and G. W. Crabtree, Phys. Rev. Lett. **80**, 1070 (1998).
- ³⁶W. Jiang, N-C. Yeh, T. A. Tombrello, R. P. Rice, and F. Holtzberg, J. Phys.: Condens. Matter **9**, 8085 (1997).
- ³⁷A. M. Petrean, L. M. Paulius, W. K. Kwok, J. A. Fendrich, and G. W. Crabtree (unpublished).
- ³⁸R. Ikeda, J. Phys. Soc. Jpn. **66**, 1603 (1997).
- ³⁹W. K. Kwok, J. A. Fendrich, C. J. van der Beek, and G. W. Crabtree, Phys. Rev. Lett. **73**, 2614 (1994).
- ⁴⁰T. Nishizaki, Y. Onodera, N. Kobayashi, H. Asaoka, and H. Takei, Phys. Rev. B **53**, 82 (1996).
- ⁴¹T. Ishida, K. Okuda, and H. Asaoka, Phys. Rev. B **56**, 5128 (1997).
- ⁴²G. W. Crabtree, W. K. Kwok, U. Welp, D. Lopez, and J. A. Fendrich, in *Physics and Material Science of Vortex States, Flux Pinning and Dynamics*, Vol. 356 of *NATO Advanced Study Institute, Series E: Applied Sciences*, edited by R. Kossowsky et al. (Kluwer Academic Publisher, Dordrecht, 1999), p. 357.